

First-Principles Quantum Dynamics of Singlet Fission: Coherent versus Thermally Activated Mechanisms Governed by Molecular π Stacking

Hiroyuki Tamura,^{1,*} Miquel Huix-Rotllant,² Irene Burghardt,² Yoann Olivier,³ and David Beljonne³

¹WPI-Advanced Institute for Material Research, Tohoku University, 2-1-1 Katahira, Aoba-ku, Sendai 980-8577, Japan

²Institute of Physical and Theoretical Chemistry, Goethe University Frankfurt, Max-von-Laue-Straße 7, 60438 Frankfurt am Main, Germany

³Laboratory for Chemistry of Novel Materials, University of Mons, Place du Parc 20, 7000 Mons, Belgium

(Received 16 April 2015; revised manuscript received 4 June 2015; published 31 August 2015)

Singlet excitons in π -stacked molecular crystals can split into two triplet excitons in a process called singlet fission that opens a route to carrier multiplication in photovoltaics. To resolve controversies about the mechanism of singlet fission, we have developed a first principles nonadiabatic quantum dynamical model that reveals the critical role of molecular stacking symmetry and provides a unified picture of coherent versus thermally activated singlet fission mechanisms in different acenes. The slip-stacked equilibrium packing structure of pentacene derivatives is found to enhance ultrafast singlet fission mediated by a coherent superexchange mechanism via higher-lying charge transfer states. By contrast, the electronic couplings for singlet fission strictly vanish at the C_{2h} symmetric equilibrium π stacking of rubrene. In this case, singlet fission is driven by excitations of symmetry-breaking intermolecular vibrations, rationalizing the experimentally observed temperature dependence. Design rules for optimal singlet fission materials therefore need to account for the interplay of molecular π -stacking symmetry and phonon-induced coherent or thermally activated mechanisms.

DOI: 10.1103/PhysRevLett.115.107401

PACS numbers: 78.55.Kz, 78.20.Bh, 78.47.da, 82.20.Gk

Singlet excitons in various molecular systems including π -conjugated molecular crystals and semiconducting polymers can split into two triplet excitons following a spin-conserving process denoted singlet fission [1–13]. When combined with a suitable acceptor material, the triplet excitons subsequently produce charge-separated electron-hole pairs that can create a photocurrent. Hence, singlet fission has attracted much attention lately in the context of photovoltaics, where internal quantum efficiencies in excess of 100% have been produced due to the effective carrier multiplication [4]. As triplet excitons usually diffuse over longer distances ($\sim \mu\text{m}$) compared to singlets [2,3], singlet fission can also be implemented in thick multilayer architectures. Differently from ordinary singlet-triplet conversions via slow intersystem crossings, singlet fission can be ultrafast under certain conditions, exceeding the rate of other competing processes. Among different classes of π -conjugated molecules, acenes were identified early on as singlet fission materials [1], where tetracene and pentacene are favorable in terms of energetics, but anthracene is not [Fig. 1(c)]. Beyond simple energetics, much work is in progress to elucidate the microscopic mechanism of singlet fission.

Transient absorption spectroscopy investigations point to an ultrafast singlet fission process in molecular crystals of pentacene [5] and its derivative 6,13-bis(triisopropyl-silyl-ethynyl)-pentacene (TIPS-pentacene) [13]. Contradicting views on the mechanistic aspects of singlet fission have been reported in the literature [8–10]. Briefly, it has been

proposed that singlet fission either proceeds through a direct two-electron coupling between the singlet exciton (XT) and the triplet pair (TT) or follows an indirect mechanism where charge-transfer (CT) states act as virtual mediating states (i.e., superexchange) or are transiently populated. In both cases, the singlet-triplet conversion is believed to be driven by coupling to nuclear degrees of freedom and involves either a conical intersection or an avoided crossing pathway. Very interestingly, recent two-pulse time resolved transient spectroscopy experiments performed on TIPS-pentacene thin films have demonstrated that (i) while light absorption does not directly generate a coherent superposition of XT and TT at time zero, the TT population grows in time at the expense of XT with an 80 fs time constant, and that (ii) yet, the vibrational coherences generated upon photoexcitation into XT are largely transferred to TT during the singlet fission process [13]. This implies an essential role of electron-phonon (vibronic) coupling in the coherent singlet fission process.

In contrast to TIPS-pentacene, singlet fission in the rubrene crystal has been reported to be a thermally activated process and is characterized by a much longer time constant of few ps [7]. The driving force from a Frenkel singlet exciton to a triplet pair in rubrene is slightly exergonic at the relaxed geometries [Fig. 1(c)] [14], as is the case for tetracene that exhibits temperature-independent singlet fission [6]. Thus, the reason why only rubrene exhibits a thermally activated singlet fission cannot be explained solely by the XT-TT energetics.

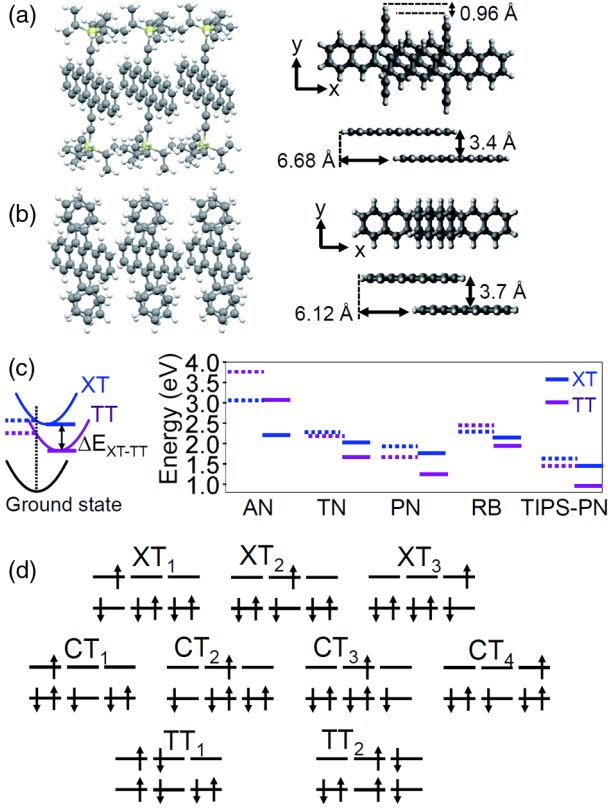


FIG. 1 (color online). (a) Crystal structure of TIPS-pentacene and the dimer model constructed for MRMP2 calculations, where the side group is simplified as alkyne. (b) Crystal structure of rubrene and the dimer model for MRMP2 calculations, where the side group is neglected. (c) Energy diagram showing the vertical (solid lines) and relaxed (dashed lines) excitation energies to the Frenkel exciton, XT (blue), and triplet pair, TT (purple), in TIPS-pentacene (TIPS-PN) and rubrene (RB), together with those of the herringbone dimers of anthracene (AN), tetracene (TN), and pentacene (PN). (d) Diagram of electron configurations of XT, TT, and CT states in the three-site, nine-state model.

In this study, we propose a nonadiabatic quantum dynamical model that describes singlet exciton fission in realistic systems through parametrizations based on highly correlated *ab initio* electronic structure calculations. Notably, we highlight a crucial role of molecular stacking symmetry in the contrasting mechanisms of singlet fission in representative molecular crystals, namely TIPS-pentacene and rubrene. We find that while the slip-stacked equilibrium structure of TIPS-pentacene is favorable for ultrafast singlet fission mediated by a coherent superexchange mechanism, singlet fission in the C_{2h} symmetric stacking of rubrene is driven by thermal excitations of symmetry-breaking vibrations.

We consider the following linear vibronic coupling Hamiltonian in a diabatic representation:

$$H = \sum_I h_I(\mathbf{x})|I\rangle\langle I| + \sum_{I>J} V_{IJ}(X)(|I\rangle\langle J| + \text{H.c.}) \quad (1)$$

with

$$h_I(\mathbf{x}) = \sum_i \frac{\omega_i}{2} (x_i^2 + p_i^2) + \sum_i \kappa_i^I x_i + E_I, \quad (2)$$

where I and J are the indices for the relevant XT, TT, and CT states. The diagonal term, $h_I(\mathbf{x})$, consists of harmonic oscillators for the intramolecular modes, x_i , where ω_i is the frequency, p_i is the momentum, κ_i^I is the vibronic coupling, and E_I is the excitation energy at the ground-state geometry. The off-diagonal term, V_{IJ} , is the electronic coupling between the states which depends on intermolecular modes, X . The multiconfiguration time-dependent Hartree (MCTDH) method [15] has been used to solve the Schrödinger equation, $i\partial\Psi/\partial t = H\Psi$, with $\Psi = \sum_I \Psi_I |I\rangle$, where Ψ_I are the vibrational wave functions on the respective electronic states. All intramolecular vibrational modes, i.e., 22 modes per molecule for TIPS-pentacene and 15 for rubrene, and selected intermolecular modes are included in the MCTDH calculations. Our model can describe coherent and incoherent singlet fission dynamics mediated by vibronic coupling of realistic systems.

We consider a molecular trimer, i.e., a three-site, nine-state model consisting of three XT, two TT, and four CT states [Fig. 1(d)] for the quantum dynamics calculations, where the Frenkel exciton on the center site (XT_2) is coupled to two TT states similar to the bulk condition. The trimer model can also describe delocalized initial excitons by setting the wave function amplitudes on the respective sites, where the bright and dark excitons are, respectively, described by identical and opposite signs of the amplitudes on neighboring sites.

The Hamiltonian matrix elements (Table I) are determined based on electronic structure calculations of the dimer models [Figs. 1(a) and 1(b)] using the multireference second order perturbation theory (MRMP2) with the correlation consistent polarized basis set (cc-pVDZ), expected to provide an accurate description of the excited states. Here, the dimer geometries are extracted from experimental single crystal structures. The XT, TT, and CT energies and their pairwise couplings are obtained by applying a unitary transformation from the dimer adiabatic electronic states to the diabatic representation [16]. The four frontier molecular orbitals, i.e., highest occupied molecular orbital (HOMO), HOMO - 1, lowest unoccupied molecular orbital (LUMO) and LUMO + 1, are considered as active orbitals in MRMP2 calculations on the dimers. The reorganization energies and the intramolecular vibronic couplings are evaluated based on the frequencies of normal modes and geometry optimizations in the respective states, using density functional theory (DFT) with the Perdew-Burke-Ernzerhof functional, where the spectral density is broadened by introducing site-specific shifts [16]. The GAMESS code [17] is used for all *ab initio* calculations.

TABLE I. Hamiltonian matrix (symmetric matrix) of singlet fission in diabatic representation where the diagonal and off-diagonal elements correspond to the vertical excitation energies and the electronic couplings (eV), respectively.

	TT ₁	TT ₂	XT ₁	XT ₂	XT ₃	CT ₁	CT ₂	CT ₃	CT ₄
TT ₁	E _{TT}	0.0	−V _{TX}	V _{TX}	0.0	V _{TC}	V _{TC}	0.0	0.0
TT ₂		E _{TT}	0.0	V _{TX}	−V _{TX}	0.0	0.0	V _{TC}	V _{TC}
XT ₁			E _{XT}	V _{XX}	0.0	−V _{HOMO}	V _{LUMO}	0.0	0.0
XT ₂				E _{XT}	V _{XX}	−V _{LUMO}	V _{HOMO}	V _{HOMO}	−V _{LUMO}
XT ₃					E _{XT}	0.0	0.0	V _{LUMO}	−V _{HOMO}
CT ₁						E _{CT}	−V _{CC}	−V _{CC}	0.0
CT ₂							E _{CT}	0.0	−V _{CC}
CT ₃								E _{CT}	−V _{CC}
CT ₄									E _{CT}
<hr/>									
				E _{TT}		E _{XT}		E _{CT}	
TIPS-pentacene				1.469		1.618		1.992	
Rubrene				2.451		2.311		3.097	
<hr/>									
		V _{TX}		V _{TC}		V _{XX}		V _{HOMO}	
TIPS-pentacene		0.013		0.084		0.018		0.041	
Rubrene		0.0		0.0		0.079		−0.175	
<hr/>									

First, we address singlet fission in TIPS-pentacene. Table I shows the diabatic state energies and electronic couplings, as obtained from MRMP2 calculations in the ground-state geometry. Accounting for the intramolecular reorganization energy from the ground state to the exciton ($\lambda_{XT} = 0.15$ eV) and TT ($\lambda_{TT} = 0.45$ eV) state geometries, the driving force ΔE_{XT-TT} amounts to -0.45 eV.

The slip-stacked configuration of TIPS-pentacene results in large electronic couplings for both the direct and CT-mediated pathways (Table I). Accordingly, the quantum dynamics simulations point to an ultrafast singlet fission with a time scale of ~ 100 fs (Fig. 2), in very good agreement with experimental data [13]. The contributions arising from the two channels can be clearly disentangled by accounting for only one of either the direct two-electron XT-TT coupling or the indirect XT-CT and CT-TT couplings [Figs. 2(b) and 2(c)]. Even though the intermediate CT states are ~ 0.4 eV higher in energy than the initial exciton state in our calculations, the superexchange pathway is found to promote an ultrafast singlet fission process and dominates over the direct mechanism in the first 100 fs. Such a coherent superexchange cannot be described by perturbative hopping pictures, highlighting the importance of nonadiabatic quantum dynamical treatments. Note that the picture above is not affected by initial excitation conditions; i.e., very similar results are obtained when preparing the system either in a localized Frenkel exciton or in a delocalized (bright or dark) exciton state [Figs. 2(a), 2(d), and 2(e)]. Besides, the ultrafast singlet fission in TIPS-pentacene is robust against ΔE_{XT-TT} as long as the system is exergonic [16].

The coherent nature of singlet fission in TIPS-pentacene is analyzed based on the overlap of vibronic wave packets on the XT and TT states [18]. The substantial vibronic coherence during the first ~ 100 fs [Fig. 3(a)] indicates that the wave packet prepared on the XT potential energy surface is only weakly perturbed upon crossing onto the TT hypersurface, in line with the coherent nature of the process revealed in the transient spectroscopy experiments [13]. Here, the intramolecular vibronic coupling mediates resonance between the initial and final states, and thus purely electronic models cannot correctly describe the singlet fission process [16]. The spread of the wave packet on the XT potential surface is wide enough to cross the XT-TT avoided crossing immediately after the excitation from the ground state [Fig. 3(b)], hence rationalizing the coherence transfer via the direct pathway [Fig. 3(a)]. Our analysis further shows that the vibronic coherence is transferred throughout the superexchange pathway even via the higher-lying CT states [Fig. 3(a)] owing to the strong electronic couplings.

Next, we investigate the origin for the reported thermally activated singlet fission process in rubrene crystals. Singlet fission in rubrene is exergonic ($\Delta E_{XT-TT} = -0.21$ eV) when accounting for the reorganization energies ($\lambda_{XT} = 0.18$ eV and $\lambda_{TT} = 0.53$ eV). Remarkably, the TT-XT and TT-CT couplings are strictly zero at the C_{2h} equilibrium geometry of rubrene (V_{TX} and V_{TC} in Table I). In the adiabatic representation, the C_{2h} π stacking corresponds to a conical intersection (zero-gap seam) [20], and the vibronic couplings of symmetry-breaking modes induce an avoided crossing between the adiabatic states [Fig. 4(c)]. We show below that such a symmetry-breaking

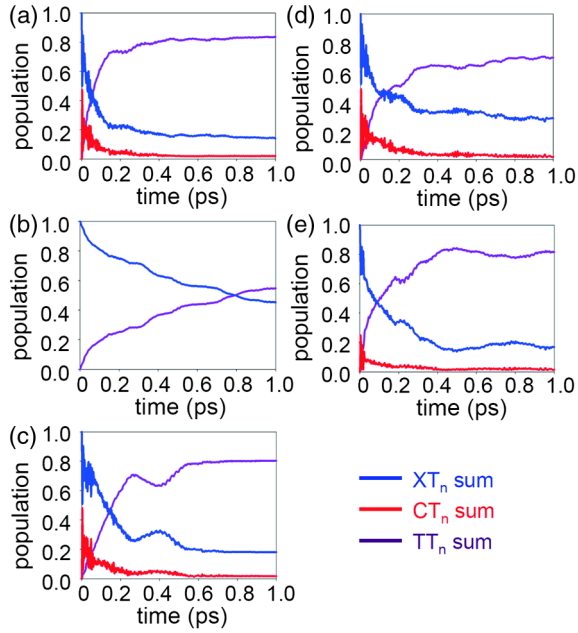


FIG. 2 (color online). Cumulative populations of XT_n (blue), CT_n (red), and TT_n (purple) in the quantum dynamics calculations of singlet fission in TIPS-pentacene. (a) Initial exciton is localized on the center molecule (XT_2), and all electronic couplings are considered. Only one of (b) direct and (c) CT-mediated pathways are considered. Dynamics from (d) bright delocalized exciton with the initial amplitude $(XT_1, XT_2, XT_3) = (1/\sqrt{3}, 1/\sqrt{3}, 1/\sqrt{3})$, and from (e) dark exciton, $(XT_1, XT_2, XT_3) = (1/\sqrt{3}, -1/\sqrt{3}, 1/\sqrt{3})$.

mechanism involves relative intermolecular displacements along the rubrene short axis. This argument also holds for the D_{2h} stacking [11].

We therefore calculated the potential energy curve and the TT-XT and TT-CT electronic couplings with respect to

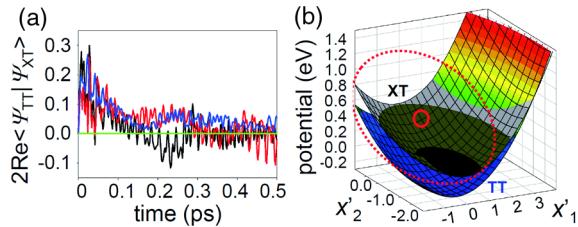


FIG. 3 (color online). (a) Overlap integral $\langle \Psi_{TT} | \Psi_{XT} \rangle$ of vibrational wave packets on the XT and TT states during singlet fission in TIPS-pentacene (black), and those considering only the direct (blue) and superexchange (red) pathways, where the initial exciton is localized on XT_2 . The overlap for rubrene (green) is negligibly small. (b) Potential energy surface of TT (color) and XT (gray scale) states of TIPS-pentacene in an effective-modes (x'_1, x'_2) representation [19]. The solid and dashed red circles indicate the Frank-Condon region from the ground state and the spread of the wave packet, respectively.

the displacement along the short axis [Figs. 4(a) and 4(b)], using DFT with the B3LYP functional and Grimme's dispersion correction [21]. From the linear dependence of the electronic coupling with displacement, one can extract the corresponding off-diagonal (nonlocal) electron-phonon coupling, $V_{IJ} = \lambda_{IJ}X$ ($\lambda_{TT-XT} = 0.002$ eV, $\lambda_{TT-CT} = 0.003$ eV), while a harmonic fit of the ground-state potential energy curve yields the frequency (~ 0.007 eV) of the intermolecular symmetry-breaking mode, X .

Quantum dynamics simulations have been performed by including in the Hamiltonian the symmetry-breaking intermolecular mode in addition to the intramolecular modes. Temperature effects are built in by considering populations of the initial vibrational excitations

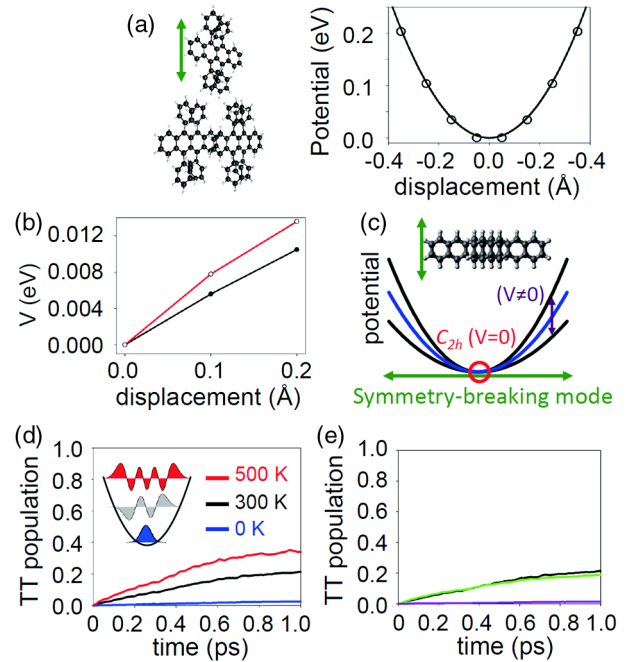


FIG. 4 (color online). (a) Potential curve with respect to displacement along the short molecular axis as obtained from DFT calculations of three rubrene molecules extracted from the crystal. To account for the steric hindrance from the other side of the molecular layer, the mirror image of the calculated potential curve is added. (b) TT-XT (black) and TT-CT (red) electronic couplings by MRMP2. (c) Schematic illustration of the conical intersection at the C_{2h} π stacking (red circle) and the avoided crossing due to symmetry breaking, where the black and blue parabolas illustrate the adiabatic potentials and the seam of diabatic potentials, respectively. (d) TT population during singlet fission in rubrene considering a bright initial exciton. Two intermolecular modes (connecting sites 1 and 2, and sites 2 and 3, respectively) are considered, where $\langle N_{\text{phonon}} \rangle$ are zero (blue), three (black), and six (red). (e) The black line is identical to that in Fig. 4(d), which is compared with TT evolution considering only one of the direct (green) and superexchange (purple) pathways.

(i.e., phonon number, N_{phonon}) of the symmetry-breaking mode from the Bose-Einstein distribution, $\langle N_{\text{phonon}} \rangle = 1/\{\exp(\beta\omega) - 1\}$, where β is the inverse temperature. Our quantum dynamics calculations indicate an increase in the singlet fission rate with increasing temperature [Fig. 4(d)], consistent with the measured thermally activated behavior [7]. At 0 K, the vibrational wave function is localized around the C_{2h} region where singlet fission is inefficient, since the off-diagonal vibronic couplings ($\lambda_{\text{TT-XT}}$ and $\lambda_{\text{TT-CT}}$) are small in this system. At higher temperatures, the symmetry-breaking mode broadens the wave packet over a region where the couplings, $V_{\text{TX}}(X)$ and $V_{\text{TC}}(X)$, become large. In contrast to TIPS-pentacene, singlet fission in rubrene is (i) incoherent [Fig. 3(a)], (ii) mediated by the direct two-electron transition with negligible contribution from the superexchange pathway [Fig. 4(e)], and (iii) occurs around a conical intersection with the wave packet on TT being affected by destructive interference due to the Berry phase [16,20].

In summary, we have proposed a nonadiabatic quantum dynamical model of singlet exciton fission fully parametrized against first principles calculations. This model was applied to resolve the current controversy about the mechanisms underlying the ultrafast and thermally activated singlet fission in representative π -stacked molecular crystals. The present analysis provides conclusive evidence that in TIPS-pentacene both the direct and superexchange pathways mediate singlet fission via an avoided crossing. Notably, the coherent singlet fission via higher-lying charge transfer states and its dominant contribution to the ultrafast dynamics are not intuitively obvious without the explicit quantum dynamical analysis. While the slip-stacked TIPS-pentacene results in strong electronic couplings with the triplet pairs, these vanish at the equilibrium C_{2h} stacking of rubrene. Our calculations indicate that singlet fission in rubrene is driven by thermal excitations of symmetry-breaking vibrations which enhance the thermally averaged electronic couplings. This picture is generally applicable for parallel π -stacked molecules, while tetracene and pentacene crystals exhibit nonzero electronic couplings for singlet fission at the equilibrium herringbone packing configurations. Molecular design rules for controlling singlet fission should thus account for packing symmetry in conjunction with phonon-induced coherent or thermally activated mechanisms.

H. T. acknowledges support from an Invited Professor Fellowship, FNRS, Belgium. The Advanced Institute for Materials Research (AIMR) is supported by World Premier International Research Center Initiative (WPI), MEXT, Japan. D. B. acknowledges support as an FNRS Research Fellow. M. H.-R. acknowledges a fellowship

within the postdoctoral program of the Alexander von Humboldt foundation. Support by the Deutsche Forschungsgemeinschaft (DFG) in the framework of Project No. BU-1032-2 is gratefully acknowledged.

*Corresponding author.

hiroyuki@wpi-aimr.tohoku.ac.jp

- [1] M. B. Smith and J. Michl, *Chem. Rev.* **110**, 6891 (2010).
- [2] H. Najafov, B. Lee, Q. Zhou, L. C. Feldman, and V. Podzorov, *Nat. Mater.* **9**, 938 (2010).
- [3] P. Irkhin and I. Biaggio, *Phys. Rev. Lett.* **107**, 017402 (2011).
- [4] D. N. Congreve, J. Lee, N. J. Thompson, E. Hontz, S. R. Yost, P. D. Reusswig, M. E. Bahlke, S. Reineke, T. Van Voorhis, and M. A. Baldo, *Science* **340**, 334 (2013).
- [5] M. W. B. Wilson, A. Rao, J. Clark, R. S. S. Kumar, D. Brida, G. Cerullo, and R. H. Friend, *J. Am. Chem. Soc.* **133**, 11830 (2011).
- [6] M. W. B. Wilson, A. Rao, K. Johnson, S. Gélinas, Riccardo di Pietro, J. Clark, and R. H. Friend, *J. Am. Chem. Soc.* **135**, 16680 (2013).
- [7] L. Ma, K. Zhang, C. Kloc, H. Sun, C. Soci, M. E. Michel-Beyerle, and G. G. Gurzadyan, *Phys. Rev. B* **87**, 201203 (2013).
- [8] P. M. Zimmerman, Z. Zhang, and C. B. Musgrave, *Nat. Chem.* **2**, 648 (2010).
- [9] D. Beljonne, H. Yamagata, J. L. Bredas, F. C. Spano, and Y. Olivier, *Phys. Rev. Lett.* **110**, 226402 (2013).
- [10] S. R. Yost *et al.*, *Nat. Chem.* **6**, 492 (2014).
- [11] T. C. Berkelbach, M. S. Hybertsen, and D. R. Reichman, *J. Chem. Phys.* **138**, 114103 (2013); *J. Chem. Phys.* **141**, 074705 (2014).
- [12] P. B. Coto, S. Sharifzadeh, J. B. Neaton, and M. Thoss, *J. Chem. Theory Comput.* **11**, 147 (2015).
- [13] A. J. Musser, M. Liebel, C. Schnedermann, T. Wende, T. B. Kehoe, A. Rao, and P. Kukura, *Nat. Phys.* **11**, 352 (2015).
- [14] Note that XT in Fig. 1(c) indicates the diabatic energy of a localized (Frenkel) singlet exciton. Delocalization of the singlet exciton can change the energetics; e.g., bright and dark excitons are higher and lower in energy, respectively.
- [15] H. D. Meyer, U. Manthe, and L. S. Cederbaum, *Chem. Phys. Lett.* **165**, 73 (1990); The MCTDH Package, Version 8.5, 2014, <http://www.pci.uni-heidelberg.de/tc/usr/mctdh/>.
- [16] See Supplemental Material at <http://link.aps.org/supplemental/10.1103/PhysRevLett.115.107401> for further detail.
- [17] M. W. Schmidt *et al.*, *J. Comput. Chem.* **14**, 1347 (1993).
- [18] O. V. Prezhdo and P. J. Rossky, *Phys. Rev. Lett.* **81**, 5294 (1998).
- [19] H. Tamura, J. G. S. Ramon, E. R. Bittner, and I. Burghardt, *Phys. Rev. Lett.* **100**, 107402 (2008).
- [20] *Conical Intersections: Theory, Computation, and Experiment*, Advanced Series in Physical Chemistry, Vol. 17, edited by W. Domcke, D. R. Yarkony, and H. Köppel (World Scientific, Singapore, 2011).
- [21] S. Grimme, *J. Comput. Chem.* **27**, 1787 (2006).